Simple model for the polarization reversal current in a ferroelectric liquid crystal

I. Dahl, S. T. Lagerwall, and K. Skarp
Department of Physics, Chalmers University of Technology, S-412 96 Göteborg, Sweden
(Received 14 January 1987)

The spontaneous ferroelectric polarization in the chiral smectic-*C* phase can be measured by monitoring the dynamic response to a changing electric field. A model for the system is presented and analyzed for the two cases of square-wave and sinusoidal voltage applied to a "bookshelf geometry" sample, where the smectic layers are oriented relative to the glass plates as books are to a shelf. The model gives a good description for the observed polarization reversal current and yields the rotational viscosity and one effective elastic constant in addition to the spontaneous polarization. Relations between these parameters and the width of the observed hysteresis loop are derived as well as relations for the contribution of the ferroelectric polarization to the permittivity. The model is applied in evaluating data from measurements on the substance MBRA-8 [2-hydroxy-4(2-methyl-butyloxy)-benzylidene-4-*p*-*n*-octyl-aniline].

I. INTRODUCTION

Ferroelectric liquid crystals in thin cells have a big potential electro-optic applicability, and it is presently of great interest to further increase our structural knowledge of the properties of such systems. In the present work we have studied thin planar cells with chiral smectic-*C* liquid crystal in the bookshelf geometry,[1] and investigated the polarization reversal current in these samples. We have made a model that describes the experimental behavior of the polarization reversal and calculated the shape of the current bump for the case of applied square-wave voltage, using a small number of parameters that are adequate for the experimental evaluation of the curves. Knowledge of the expected shape makes the experimental evaluation easier, especially in nonideal situations, and it also illuminates the physics of the process. A particular feature of the model is that it can account for the time delay between the field reversal and the current peak.

In the first described surface-stabilized ferroelectric liquid-crystal (SSFLC) cells,[2] director and polarization fields were described to be uniform in space, giving rise to the existence of the two polarization states up and down. It seems that in the measuring cells used in this work, the field-free state is rather of an optically twisted conformation with polar boundary conditions,[3] and our model is chosen accordingly. Evidence for this type of conformation is given in Sec. XIII. It is generally difficult to experimentally determine the exact director configuration in very thin SSFLC cells. One must therefore often use indirect indications such as electrical response or symmetry considerations in order to establish a model for the director and polarization profiles. As it turns out, however, our model does not depend on assumptions of the exact boundary conditions of the cell. Rather an effective elastic term is introduced in the model, giving the model a much broader field of applicability than one requiring the boundary conditions as input parameters.

To test the applicability of the model, measurements on the substance MBRA-8 [2-hydroxy-4(2-methyl-butyloxy)-benzylidene-4-*p*-*n*-odyl-aniline] have been reevaluated. We discuss below the limits of the model and investigate also its consequences in the case of a sinusoidal driving voltage. We thus obtain an expression for the width of the ferroelectric hysteresis loop in some limits.

One method to measure the ferroelectric polarization is to apply a square-wave voltage and measure the polarization reversal current through the cell.[4] The observed current between the capacitor plates is, however, not identical to the polarization reversal current. We will, in general, get four contributions to the observed current.

The first part is the dielectric charging and discharging of the capacitor formed by the electrodes on the boundary plates of the cell. This contribution gives an exponentially decaying current after each voltage reversal, where the time constant can be lowered by decreasing the resistance of the electrodes.

The second part (often hidden inside the first) comes from the electroclinic effect.[5] This effect gives a linear increase or decrease in the tilt angle in response to the applied electric field. Since the response is linear and only one viscosity coefficient should be involved, this should also give an exponentially decaying current if it can be separated in time from the polarization reversal. It should be of small amplitude and with a time constant that only depends on temperature and on liquid-crystal material parameters. The electroclinic part may be expected to play a role in the immediate vicinity of the smectic-*C*-to-smectic-*A* transition and might complicate the evaluation there.

The third part is the polarization reversal current, giving a typical "bump" in the current. The area of this bump is proportional to the magnitude of the polarization.

The fourth part is of electrolytic origin. Dissolved charged impurities move from one electrode to the other and may also participate in electrode reactions. In some

cases this can give current shapes similar to the polarization reversal current. By use of pure material, and by proper choice of time scale and switching voltage, this contribution can mostly be reduced to a simple shift in the base line. A polarization reversal current bump can easily be distinguished from an electrolytic current bump by checking the optical repsonse and the behavior with raising temperature.

A benefit of using a square-wave voltage compared to other driving voltage shapes is that we in most cases can get a time separation of the four above-mentioned contributions, which not only facilitates the extraction of a correct polarization value together with information on viscosity and elasticity, but also yields some test factors relating to the condition of the specimen (e.g., resistivity).

II. MODEL ASSUMPTIONS

A leading principle has been to find a model that permits analytic solutions, since this permits easy use of the solution as an evaluation tool for experimental measurements. In order to keep the mathematics simple with a low number of free parameters, we have chosen to describe a clearcut experimental case. We will later also discuss how to handle other more complicated cases.

We assume that we can let one single angle ϕ represent the direction of the spontaneous polarization in the whole sample. That does not mean that there are no deformations in boundary layers or near defects; we only assume that their contributions to the current are negligible. We restrict our description to the low-voltage range, where elastic deformation can be expected to dominate over creation and motion of disclinations and over inelastic changes at the electrodes. We are thus well below the limit for bistable switching. We also ignore flexoelectric effects and the effects of variation in the dielectric constant during the polarization reversal. If there should be a difference between the two dielectric constants parallel to the smectic layers, this could change the shape of the current bump, but would not change the area beneath it. This anisotropy seems to be small in most cases, and it seems difficult to differentiate between effects from this source and effects from inhomogeneous orientation without independent knowledge of the size of the anisotropy. Assume further that the normal of the smectic layers lies in the plane of the electrodes and that the polarization makes an angle ϕ with the normal to the electrodes (see Fig. 1).

We assume a viscous torque working against the reorientation of the polarization in an electric field and we assume it to be simply proportional to the time derivative of ϕ. As will be discussed more later, we must introduce an elastic torque, which is nonzero for the ϕ values 0 and π, in order to explain the observed finite polarization reversal times. In our monostable cells we have symmetric response with respect to the sign of the applied voltage. This indicates that the elastic equilibrium angle for ϕ in $\pi/2$, which maybe can seem surprising to some people. But this choice is the only one allowed by symmetry (except for added multiples of π), and we will below give arguments for it. Our elastic torque must be

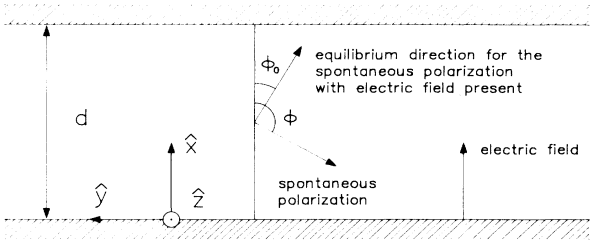

FIG. 1. Geometry of the planar cell with definition of angles and coordinates. The smectic planes are parallel to the plane of the paper.

chosen accordingly. The simple choice that we have made is that the elastic torque is proportional to $\cos\phi$. This expression for the elastic torque has been chosen, out of many possibilities, for its mathematical simplicity, and could be considered as the first term in a more general series expansion, or an approximation of the effects of elastic terms from deformations near or at the boundaries. There is a number of different boundary conditions that could give such a behavior as this elastic term indicates. The conceptually simplest case is to have boundary conditions that force the polarization to point parallel to the glass plates, see Fig. 2(a). Another quite different situation with symmetric response is the case of strongly polar boundary conditions $\phi=0$ and π, respectively, as illustrated in Fig. 2(b). The conformation in our cells is probably somewhat in between, as discussed in Sec. XIII. (If we would study cells with other boundary conditions, without symmetric response, we should in most cases expect a very similar behavior to our special cells as soon as the electrical forces dominate over the weak elastic forces, even if we should have movements of disclinations or inelastically changing boundary conditions. For this general case, it can be interesting to be able to measure the shape of the elastic potential and in Sec. XIV we have indicated how.)

Besides boundary conditions, another possible source to the elastic term may be deformed smectic layers. The same kind of symmetry arguments should be applicable for this possibility.

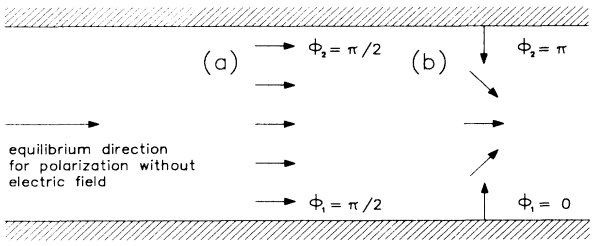

FIG. 2. Two cases giving elastic equilibrium angle $\pi/2$: (a) Uniform orientation of the polarization between the electrodes, boundary conditions $\phi_1=\phi_2=\pi/2$ and (b) strongly polar boundary conditions, boundary conditions $\phi_1=0$, $\phi_2=\pi$. In this case ϕ will represent the average direction of the polarization. For zero electric field we get $\phi=\pi/2$. Compare this figure with Fig. 8.

A simple torque balance (for a unit volume) then gives

$$-PE\sin\phi + K\cos\phi = \gamma\dot{\phi} \ , \tag{1}$$

where P is the ferroelectric polarization, E is the applied electric field, K is an effective elastic constant, and γ is a rotational viscosity. The elastic constant K should be dependent on the thickness d of the sample. If the elasticity has its origin in elastic boundary conditions or in boundary layers of constant thickness (independent of d), K should be proportional to d^{-1}, but if elasticity stems from boundary layers that take a fix proportion of the sample thickness, K instead should be proportional to d^{-2}. A study of K as function of the sample thickness could thus tell us something about the nature of the boundary condition.

III. SOLUTION TO THE DIFFERENTIAL EQUATION

The left-hand side of Eq. (1) can be rewritten as

$$-N\sin(\phi-\phi_0) \ , \tag{2}$$

where

$$N=[(PE)^2+K^2]^{1/2} \quad \text{and} \quad \sin\phi_0 = K/N \ . \tag{3}$$

Equation (1) is identical to the equation for an overdamped pendulum with the equilibrium angle ϕ_0,

$$\kappa\sin(\phi-\phi_0) = -\dot{\phi} \ , \tag{4}$$

with

$$\kappa = N/\gamma \ . \tag{5}$$

The electric current due to the polarization reversal is equal to the time derivative of the polarization charge times the electrode area A,

$$I = A\frac{d}{dt}(P\cos\phi) = -AP\dot{\phi}\sin\phi \ . \tag{6}$$

By use of Eq. (4), we get the alternative expression

$$I = AP\kappa\sin\phi\sin(\phi-\phi_0) \ . \tag{7}$$

The benefit of this simple model is that there is an analytic solution to the differential equation (4). We assume that P, E, and K are positive, and look for solutions where ϕ is starting in the second quadrant and ending up in the first. A particularly simple solution is obtained if we define t_0 as the time when ϕ takes the value $\phi_0+\pi/2$. Then by separation of variables and integration we obtain

$$\kappa(t_0-t) = \ln\tan[(\phi-\phi_0)/2] \ . \tag{8}$$

This can be inverted to give the solution to our differential equation,

$$\sin(\phi-\phi_0) = 1/\cosh[\kappa(t-t_0)] \ . \tag{9}$$

IV. CHARACTERISTIC FREQUENCY

There are several interesting things with this solution. First we observe that there is a characteristic time $1/\kappa$ that together with ϕ_0 completely describes the dynamic behavior. When the voltage decreases to zero, κ will approach the finite value

$$\kappa_0 = K/\gamma \ . \tag{10}$$

This frequency can be determined by measuring K and γ at finite voltages. It should depend both on the material used and (via K) on the sample thickness. We will see later that this parameter also will show up in the dielectric response of the sample.

V. SINGULAR BEHAVIOR WITHOUT ELASTIC RESTORING FORCE

Next we note the singular behavior for the case $K=0$. Then also ϕ_0 is zero, and we will get an unstable equilibrium position for ϕ equal to π. An initial value $\pi-\delta$ will give a polarization reversal time that increases logarithmically with $1/\delta$. In reality we always have finite reversal times, and in order to get a theory that also works in practice, we must thus include the strongest factor that disturbs the perfect alignment $\phi=\pi$, even if that factor is much smaller than electric torques. We have considered the elastic forces from the boundaries to be this strongest factor. Another possible candidate would be destabilizing flexoelectric effects, causing field-dependent boundary conditions. We postpone the discussion about this possibility to another occasion. In a paper on the problem of switching bistable ferroelectric cells, Schiller[6] has proposed fluctuations as a source of misalignment causing finite reversal times. We doubt that it in reality is possible to get such a perfect orientation that the fluctuations dominate over the static deformations caused by imperfections in the boundary conditions. Evidently, the divergent dependence on δ makes the polarization reversal method very sensitive to the configuration of the liquid crystal, and suitable for the study of boundary conditions.

One way of getting around the divergency problem without introducing an elastic force would be to insert some arbitrarily chosen nonzero initial angle ϕ_0 to get the solution. This method is not good, since it does not tell us how to choose ϕ_0, and besides that, the method will only work for the first half-period of applied voltage.

VI. METHOD FOR THE EVALUATION OF MEASURED POLARIZATION REVERSAL CURVES

Knowledge of the analytical shape of the ideal polarization reversal curve gives us alternative ways to evaluate polarization, as well as viscosity and elastic parameters for experimental samples. To begin with we can measure the height of the current reversal peak ($I_{\max}$), the time between the voltage reversal and the current peak (τ_s), and the time for the current to decay from the peak value to half the peak value (τ_+). Sometimes we also can measure the time for the current to increase from half the peak value to the peak value (τ_-). Figure 3 illustrates these quantities. According to our model, the expressions for them are

$$I_{\max} = AP\kappa\cos^2(\phi_0/2) \ , \tag{11}$$

$$\kappa\tau_s = \ln\tan[(\phi_i-\phi_0)/2] - \ln\tan(\pi/4-\phi_0/4) , \quad (12)$$

$$\kappa\tau_+ = \ln\tan(\pi/4-\phi_0/4) - \ln\tan\{\pi/4-\phi_0/4-\arccos[\sin^2(\phi_0/2)]/4\} , \quad (13)$$

$$\kappa\tau_- = \ln\tan\{\pi/4-\phi_0/4+\arccos[\sin^2(\phi_0/2)]/4\} - \ln\tan(\pi/4-\phi_0/4) , \quad (14)$$

where ϕ_i is the initial value of ϕ, at the time when the wave is of low frequency, we may assume the angle ϕ to have reached its equilibrium value in the preceeding half-period, hence

$$\phi_i = \pi - \phi_0 . \quad (15)$$

The most favorable situation for evaluation of experiments is when the sum $(\tau_- + \tau_+)$ is measurable. Then we directly estimate κ from the relation

$$\kappa(\tau_- + \tau_+) = \ln(3+\sqrt{8}) = 1.762\,75 . \quad (16)$$

This relation follows from (13) and (14) and holds independently of the value of ϕ_0. The sum $(\tau_- + \tau_+)$ can be measured with much smaller experimental error than the individual values τ_- and τ_+, since the measurement of this sum does not require the determination of the exact position of the current peak. The position of the current peak should be more sensitive to nonuniformities in the sample than the full half-width $(\tau_- + \tau_+)$. With the estimate of κ, we can calculate $\kappa\tau_s$ from the measured value of τ_s. If ϕ_i and ϕ_0 are related according to Eq. (15), the expression (12) can be inverted to give the value of ϕ_0,

$$\phi_0 = 2\arcsin\frac{\beta-(\beta^2-2\beta+2)^{1/2}}{2(\beta-1)} , \quad (17)$$

where

$$\beta = \exp(\kappa\tau_s) . \quad (18)$$

If ϕ_0 is greater than approximately 30°, the current will be higher than half the peak value immediately on voltage reversal, and it is then impossible to measure τ_-. In that case we form the experimental quantity τ_s/τ_+. According to our model this should only depend on ϕ_0, and thus the experimental value can be used to get an estimate of ϕ_0. With this estimate, κ can be calculated from the measurement of τ_+. Even this evaluation scheme breaks down if ϕ_0 is greater than 60°. In this case there is no current maximum, instead the current will decrease monotonically with time.

When ϕ_0 and κ have been evaluated, the polarization is calculated from the value of $I_{\max}$, using Eq. (11). The quotient between K and PE is also easily extracted from the value of ϕ_0,

$$K/PE = \tan\phi_0 . \quad (19)$$

Finally, γ can be estimated from the relation

$$\frac{\gamma\kappa}{PE} = \frac{1}{\cos\phi_0} . \quad (20)$$

The relevant functions of ϕ_0 are tabulated in Table I and some calculated current wave forms for different values of ϕ_0 are shown in Fig. 4.

One of the advantages with the evaluation method presented here is that it permits estimates of the polarization even in cases where it is not possible to recover the nice full reversal current curve. The evaluation scheme is quite simple and fast. Moreover, we can extract additional important physical information out of the measurement, viz., numerical values for the rotational viscosity and for one effective elastic constant. However, since the theory behind the evaluation method simplifies matters compared with the real situation, we should compare the predicted and the observed behavior and also discuss the limits of the method.

VII. COMPARISON WITH EXPERIMENTS

To check the model we have reevaluated a set of already published measurements[7] on the substance

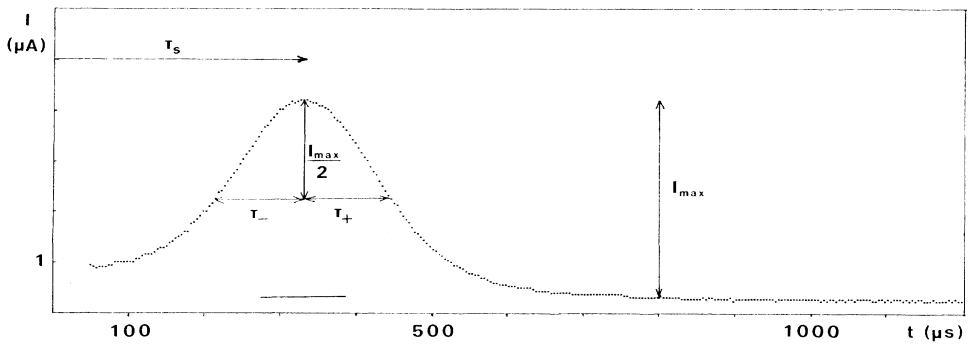

FIG. 3. A typical measured polarization reversal curve. First comes the fast exponential charging of the capacitor and then the polarization peak on top of an almost constant contribution from ionic conductance. The primary measurable quantities are indicated.

TABLE I. Parameters of the current bump as functions of ϕ_0.

ϕ_0 (degrees)	$\kappa\tau_s$	τ_s/τ_+	$\kappa\tau_+$	$I_{max}/AP\kappa$	K/PE	$\gamma\kappa/PE$
0.000 01	15.561	17.576	0.881 37	1.0000	1.75×10^{-7}	1.0000
0.0001	13.259	14.963	0.881 37	1.0000	1.75×10^{-6}	1.0000
0.001	10.956	12.433	0.881 38	1.0000	1.75×10^{-5}	1.0000
0.01	8.6535	9.8179	0.881 41	1.0000	1.75×10^{-4}	1.0000
0.1	6.3517	7.2036	0.881 74	1.0000	1.75×10^{-3}	1.0000
1	4.0569	4.5841	0.884 99	0.999 92	0.017 455	1.0002
2	3.3721	3.7949	0.888 60	0.999 70	0.034 921	1.0006
5	2.4799	2.7572	0.899 43	0.998 10	0.087 489	1.0038
10	1.8228	1.9869	0.917 41	0.992 40	0.176 327	1.0154
15	1.4482	1.5485	0.935 22	0.982 96	0.267 949	1.0353
20	1.1861	1.2449	0.952 80	0.969 85	0.363 970	1.0642
25	0.982 83	1.0132	0.970 06	0.953 15	0.466 308	1.1034
30	0.814 15	0.824 92	0.986 94	0.933 01	0.577 350	1.1547
35	0.666 67	0.664 42	1.0034	0.909 58	0.700 207	1.2208
40	0.531 80	0.521 71	1.0193	0.883 02	0.839 100	1.3054
45	0.403 20	0.389 65	1.0348	0.853 55	1	1.4142
50	0.275 45	0.262 42	1.0496	0.821 39	1.191 75	1.5557
55	0.143 15	0.134 55	1.0639	0.786 79	1.428 15	1.7434
60	0	0	1.0776	0.75	1.732 05	2

MBRA-8, made for varying voltages at the constant temperature 33.0 °C. For this substance, well-shaped current peaks are normally obtained, and there is good separation between the various current contributions. This makes it possible to compare the present evaluation method and the method of numerical integration used in the previous work. The reevaluation was enabled by the fact that previous voltage and current curves had been measured using a memory oscilloscope with an 8-bit analog-to-digital converter and then stored into a computer memory. In Fig. 5 one of the previous experimental curves is shown together with the new theoretical curve from the model.

The result of the reevaluation for various voltages is shown in Table II. For the lowest voltages applied, the current signal was too low to give good resolution of data, and these values are included here only to give a trend indication. Moreover, it was not possible to obtain any reliable value of τ_- for the two lowest voltages, so here ϕ_0 had to be estimated from the knowledge of τ_s/τ_+, which increases the uncertainties. The following can be concluded from this reevaluation.

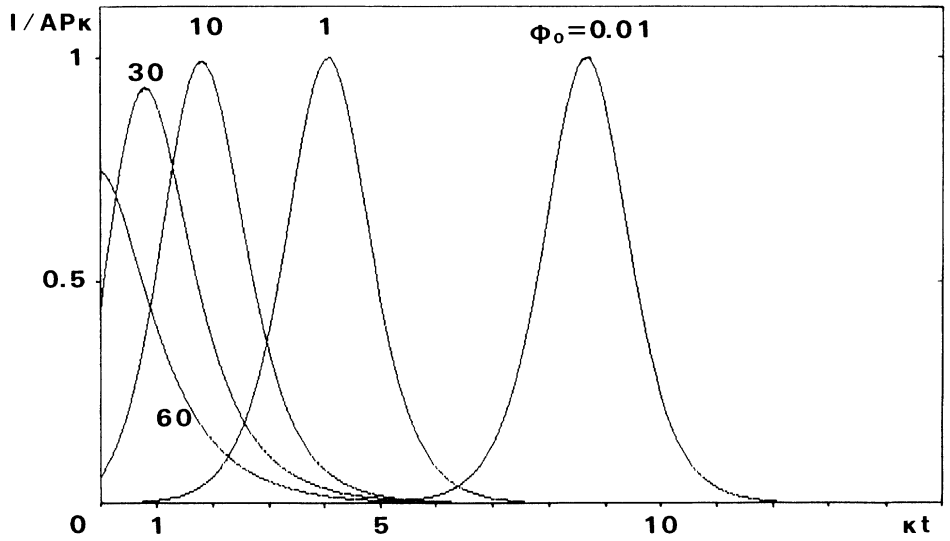

FIG. 4. Calculated current vs time for different values of the equilibrium angle ϕ_0 (0.01°, 1°, 10°, 30°, and 60°) for square-wave switching. Both variables are multiplied by constants to make them dimensionless.

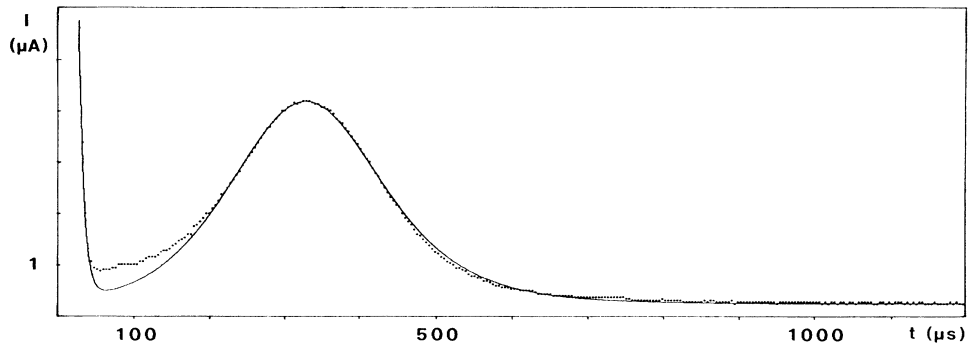

FIG. 5. Polarization reversal current curve for MBRA-8. One experimental curve (dots) and one theoretical from the model (solid).

There is very good agreement between the values of the polarization obtained using the model and using numerical integration. The variation in the new polarization values is less than or similar to the variation in the values from numerical integration. Finally, using our model we get a good estimate of the value of the polarization even at low voltages, where the switching is incomplete and the numerical integration gives too low values.

The behavior of MBRA-8 seems so far to be quite representative for most ferroelectric substances although the magnitudes of the material parameters naturally varies widely.

VIII. THE DEPENDENCY ON INITIAL CONDITIONS

The most rapid but also crudest way of estimating the rotational viscosity γ is to use dimensional analysis without considering the switching mechanism. If τ is some parameter characterizing the time required for switching, the following approximate relation can be derived,

$$\tau=\gamma/PE \ . \tag{21}$$

In dimensional analysis the correct numerical factor is lost, but the relation can anyway be interpreted to imply that the switching time should be proportional to E^{-1}.

TABLE II. Parameters obtained for MBRA-8 at 33.0 °C, varying voltages, electrode area 0.155 cm^2, and thickness 2 μm. Values in parentheses are only included to give trend indications.

	From present model					From numerical integration
Applied voltage (V)	ϕ_0 (degrees)	K ($N\,m^{-2}$)	γ[a] ($N\,s\,m^{-2}$)	κ_0 (s^{-1})	P[b] ($\mu C\,m^{-2}$)	P ($\mu C\,m^{-2}$)-
0.94	(57)	(24)	(0.028)	(857)	(33.3)	11.7
1.25	(25)	(6.8)	(0.009)	(755)	(23.5)	19.9
2.19	21.5	14.9	0.0172	866	34.5	26.0
3.28	10.8	9.4	0.0127	740	30.0	29.5
4.06	8.9	10.6	0.0152	697	33.3	32.0
5.05	6.4	9.2	0.0149	617	32.6	33.4
5.83	5.6	9.5	0.0157	605	33.3	33.9
6.77	5.8	11.8	0.0174	678	34.7	35.5
7.70	5.1	11.7	0.0177	661	34.2	35.1
8.48	5.0	12.7	0.0183	694	34.5	34.9
8.95	4.8	12.8	0.0182	703	34.4	34.9
9.58	4.7	13.4	0.0183	732	34.1	33.6
Average of extreme values excluding the first four:		11.3	0.0166	669	33.6	33.8
Max. deviation		2.1	0.0017	64	1.1	1.8

[a]Multiplication of the viscosity values by a factor of 1000 gives corresponding values in cP.
[b]$\mu C\,m^{-2}$ should be the correct Si unit for the spontaneous polarization. To get values expressed in the more commonly used unit nC/cm^2, divide the tabulated values by 10.

Measurements on the response time to electrical pulses verify that the exponent is correct,[8] but if τ_s (delay time to current peak) is used for τ in square-wave switching,[7] the exponent -0.5 seems to fit better to the experimental data in one voltage region. This indicates that the increased torque from an increased electric field must be counteracted by some other effect. Our model gives the explanation. If we study the behavior during the positive half-period of the square wave, the initial condition ϕ_i of ϕ at the switchover to positive voltage is dependent on the amplitude of the electric field during the negative half-period, i.e., a stronger negative voltage aligns ϕ_i nearer to the angle π. This will to some extent counteract the increased electric torque during the positive half-period. Evaluation of the lacking dimensionless numerical factor in Eq. (21) reveals that it goes smoothly from 0 to about 3 in the voltage range suitable for experiments and diverges logarithmically for higher voltages. The effective exponent is first positive and approaches -1 only asymptotically, values between -0.5 and -0.7 should be more typical. Our conclusion is thus that τ_s should not be used for simple estimates of the viscosity, one should instead use either the full width of the current peak at half maximum for square-wave excitation or use the response time for pulsed excitation. The parameter τ_s is instead suitable for studies of the initial conditions that could be varied by changing the driving voltage from pure square wave to more complicated shapes.

IX. OPTICAL RISE AND RESPONSE TIME MEASUREMENTS

The discussion above about the initial condition has also relevance for optical response measurements. In Fig. 6 an oscilloscope picture shows the time coincidence between the optical response and the polarization reversal current curve, measured on the same cell. According to our experience this behavior is general. For rise time of the optical response (measured for instance as the time between the 10% and 90% levels) should be proportional to the half-width of the current bump, and should thus also be proportional to the quotient between the viscosity and the polarization. The response time, measured from the voltage change to the 50% level of the optical response, could for practical purposes be considered to be identical to our parameter τ_s, and it should thus be highly dependent on the initial conditions.

X. THE LIMITATIONS OF OUR SIMPLE MODEL

A more detailed elastic theory requires more assumptions and more knowledge about the sample than we have used in our model. Anyway, it is possible to compensate to some extent for our simplifying assumptions, and we will indicate how.

We have assumed that the polarization is uniform along one direction in the whole sample. This is of course not the case in any real situation. A distribution

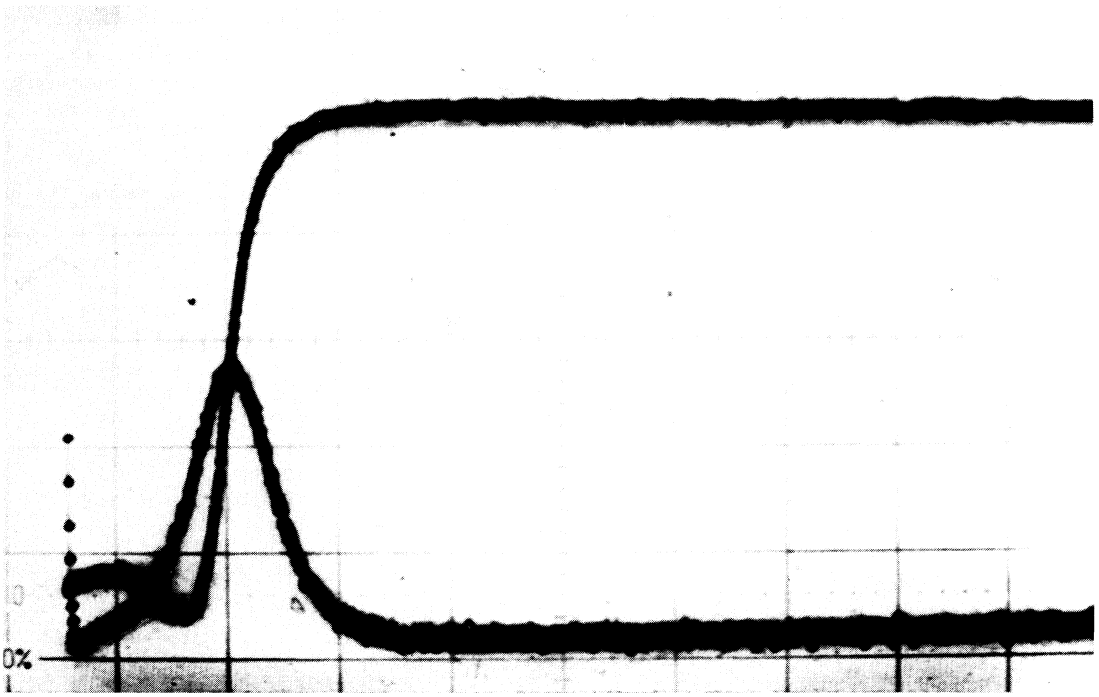

FIG. 6. An oscilloscope picture displaying the time coincidence between the electrical (current bump) and optical response (*S*-shaped curve).

of different polarization directions will give a current curve that is essentially a weighted mean of different current wave forms, where each direction of polarization contributes according to its part of the volume of the sample. This should give a broader peak than for a very well aligned sample, even if elastic forces may reduce the effect. (If the switching starts at one place, elasticity tends to propagate this behavior to the whole sample.) The broader peak yields values of the viscosity γ and also of the elastic constant K that are too high. Also there may be some boundary layers near the electrodes and around line and point defects, where the molecules do not participate at all in the switching of the polarization. The effective thickness of these layers should be inversely proportional to the strength of the applied electric field. The corresponding volumes should be proportional to $1/E$, $1/E^2$, or $1/E^3$ for planar surfaces, line defects, and point defects, respectively. Clearly, the contribution from planar surfaces will dominate if we choose the voltage high enough. If we want to study this effect, we should measure the polarization for different voltages, and plot it as a function of $1/V$. Extrapolation to $1/V=0$ could then be used to cancel the effects of the boundary layers. From Table II, we see, however, that if surface layers give a $1/V$ dependence of the polarization values, the effect in this case is smaller than the experimental errors.

When we leave the low-voltage range, the anisotropy of the dielectric constant will become important. We will get another term from the dielectric torque into our differential equation, and we will also get an extra contribution to the current from the change in capacitance during switching. We cannot, however, substitute the elastic term in our equation with the dielectric anisotropy, since the elastic force is most important in the low-voltage limit, and the dielectric contribution is most important in the high-voltage range. The dielectric term will not help against the singular behavior mentioned in Sec. V. The complete picture should of course contain both terms, but in the high-voltage range also other effects could enter.

XI. EXCITATION BY SINUSOIDAL VOLTAGE

It is intersting to apply our model to other wave forms, and we will now discuss the case of sinusoidal shape. (The case of triangular shape is easy to solve numerically, but difficult to solve analytically, and is hence not so suitable for discussion.) Here we must be more cautious in using the theory on real cells, since we can expect surface irregularities and wall motions to play a more important role for sinusoidal than for square-wave voltages, since the voltage is then increased much more slowly. It is also more difficult to handle the contributions of electrolytic origin. (The same applies for the triangular voltage.) To get tractable equations we can go to the three different limits where we assume that one of the three different terms in the differential equation is small compared to the others.

First we can look at the static limit, where the viscosity plays a negligible part. There, to zeroth order in γ, ϕ becomes equal to ϕ_0, defined by Eq. (3) above, with the actual value of the electric field inserted. In this limit there is thus no hysteresis. To first order in γ, we will get

$$\sin\phi=\frac{K}{[(PE)^2+K^2]^{1/2}}+\frac{\gamma KP^2E\dot{E}}{[(PE)^2+K^2]^2}+O(\gamma^2)\ , \tag{22}$$

and

$$\cos\phi=\frac{PE}{[(PE)^2+K^2]^{1/2}}-\frac{\gamma K^2P\dot{E}}{[(PE)^2+K^2]^2}+O(\gamma^2)\ . \tag{23}$$

The order function $O(\gamma^2)$ is here used to indicate that omitted terms are comparable to γ^2 or less. For an applied electric field of

$$E=E_0\sin(\omega t)\ , \tag{24}$$

we will then get the current

$$I=\frac{AP^2K^2}{N^3}\omega E_0\cos(\omega t)+\frac{\gamma AP^2K^2\omega^2E_0^3\sin(\omega t)\cos^2(\omega t)}{N^6}+O(\gamma^2)\ . \tag{25}$$

The width of the hysteresis loop depends on the relation between PE_0 and K. For small values of PE, Eq. (23) gives the width

$$2E_0\omega\frac{\gamma}{K}+O(\gamma^2) \tag{26}$$

if we choose to have the electric field strength on the x axis for the hysteresis loop. If instead PE_0 is much bigger than K, the width instead becomes

$$2\left[\frac{\gamma K\omega E_0}{P^2}\right]^{1/3}\ . \tag{27}$$

See Fig. 7 for an illustration of these quantities.

Secondly, we look at the limit of a sufficiently small applied field [now we use the complex notation $E=E_0\exp(i\omega t)$] with a corresponding small deformation of ϕ. Using Eqs. (1) and (4), we can then easily calculate the contribution from the movement of the permanent dipoles to the current. If we compare the current with

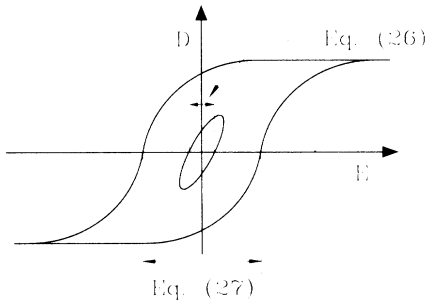

FIG. 7. Interpretation of the widths given by Eqs. (26) and (27). For small applied field, we get an elliptic figure in an E-D diagram. The width of this ellipse along the E axis is given by Eq. (26). If we increase the amplitude of the field, we get a saturated hysteresis loop, with width given by Eq. (27).

the current through an ordinary plate capacitor, we get an effective (absolute) contribution that adds to the usual dielectric constant for the liquid crystal without spontaneous polarization but in the same geometrical configuration,

$$\epsilon_{\text{chiral}}=\frac{P^2}{\gamma}\frac{\kappa_0+i\omega}{\kappa_0^2+\omega^2}\ , \tag{28}$$

where κ_0 is still defined by Eq. (10). In this context κ_0 is the cutoff frequency for excitation by low-amplitude voltage. Below this frequency, the amplitude of the response is dominated by elasticity, and the cell behaves like a capacitor, while for frequencies higher than κ_0 the viscosity limits the amplitude, and the electric response is similar to a resistor. The width of the hysteresis loop becomes very similar to expression (26),

$$2E_0\omega(\kappa_0^2+\omega^2)^{-1/2}\ . \tag{29}$$

It is not possible to extract the amplitude of the polarization from small-field measurements alone; we can only extract the proportions between P^2, γ, and K. In the small-field limit, the assumption of a constant ϕ through the sample may be too rough, and a more careful calculation requires a detailed knowledge about the ϕ values at various points in the cell.

The third limit to study is the case of a small elastic constant, which is the same as the high-frequency limit of the case when the applied field is not small. We can then assume that the only effect of the elastic term is to keep the average value of ϕ equal to $\pi/2$. The differential equation then has the analytic solution

$$\phi=2\arctan\left[\exp\left[\frac{PE_0\cos(\omega t)}{\omega\gamma}\right]\right] \tag{30}$$

and the current becomes

$$I=\frac{AP^2}{\gamma}E_0\sin(\omega t)\frac{1}{\cosh^2\left[\frac{PE_0}{\gamma}\frac{\cos(\omega t)}{\omega}\right]}\ . \tag{31}$$

If we increase the voltage from the small-amplitude limit, the current response curve will no longer be strictly sinusoidal; it will instead get a more triangular shape. Thus we will generate the third harmonics, at thrice the applied frequency. This could eventually be used for the detection of the chiral smectic-C phase. In that way we can get an electric response free of contributions from the ordinary capacitance and resistance of the cell; however, the ionic current might also generate some third harmonics.

XII. THE STATIC PERMITTIVITY

The sinusoidal case gives us the frequency dependence of ϵ_{chiral} as expressed by Eq. (28). In the zero-frequency limit this yields

$$\epsilon_{\text{chiral}}=P^2/K\ . \tag{32}$$

Except for the quadratic dependence on the spontaneous polarization, this displays how ϵ_{chiral} increases with increasing "weakness" $(1/K)$ of the medium. With $P=3.4\times10^{-5}$ C m^{-2} and $K\approx10$ N m^{-2} from Table II we obtain a permittivity value of about 10^{-10}. F/m or a relative dielectric constant of about 11. We are not aware of any dielectric measurements on MBRA-8, but an orientational contribution from the spontaneous polarization of this order of magnitude seems very reasonable. The permittivity should be dependent on cell geometry (via K).

XIII. POSSIBLE BOUNDARY CONDITIONS OF OUR CELLS

In the cells used for our polarization measurements, it is difficult to specify in the experimental situation what the boundary conditions really are. We can, however, give three arguments that point in the direction of polar boundary conditions.

First, in the measuring cells we use a thin protective layer of orthogonally evaporated SiO on the electrodes (to avoid electric breakdown). We thus have no preferential direction defined in the boundary plane. We then have both "layer normal symmetry" and "in-layer symmetry" of the boundary conditions, as defined in Ref. 1. That means that we can exchange the boundary plates either by rotation 180° around the smectic normal or by rotation 180° about an axis parallel to the smectic layers, without affecting the boundary conditions. If the boundary conditions are nondegenerate, the only possible boundary condition is with the polarization orthogonal to the boundaries, pointing either into or out from the liquid crystal in the same way on both plates (polar boundary conditions). We should thus roughly have the situation sketched in Fig. 2(b).

Secondly, the electrical measurements reveal a response that is symmetric with respect to the polarity of the applied electric field. This together with the absence of voltage thresholds is consistent with polar boundary conditions. With polar boundary conditions an arbitrarily small field should cause elastic deformation.

Finally, in the absence of the electric field, our cells mostly do not give extinction between crossed polarizers. This behavior can be expected from polar boundary conditions (and from most other nonuniform conformations). On the other hand, uniform orientation through the cell from the lower boundary to the upper boundary should always give some good extinction position. If we do not find any such position, several alternative explanations of the behavior can be ruled out.

If, however, the elasticity of the sample can affect the boundary conditions, the picture could be slightly modified. The conformation of the liquid crystal cannot be symmetric with respect to 180° rotation around the smectic normal if there are polar boundary conditions, so this symmetry of the boundary condition will be spontaneously broken. The elastic energy of the sample will decrease if the difference in angle between the two boundary conditions is diminished from 180° to a lower value, so that the polarization will display oblique angles at the boundaries. (This could go very well along with a

tilting of the smectic layers.) The self-energy of the spontaneous polarization could cause the elastic deformation to be confined to thin boundary layers,[9,10] and this could enhance the effect of elasticity. If we now try to sum up all the arguments, we should in our cells have the situation displayed in Fig. 8; unfortunately, we cannot give any numerical comparison between the strength of the boundary conditions and the bulk elasticity of the liquid crystal.

If the conclusion about polar boundary conditions is correct, cells with this surface treatment are not useful for bistable switching by electric fields, at least as long as we do not include inelastic changes at the electrodes by the electric field. This agrees with our experimental experience: To get good bistability other surface treatments should be used.

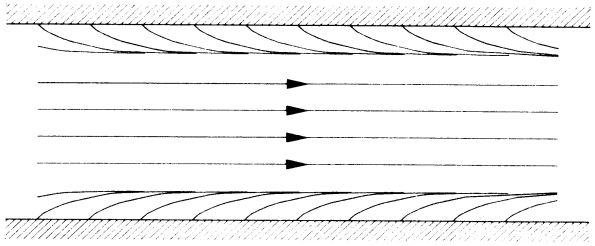

FIG. 8. The most probable conformation of our cells in the absence of applied electric field. The arrows point in the direction of the spontaneous polarization. The deformations are probably confined to two boundary layers, and the elastic forces will to some degree force the boundary conditions to be oblique and not perfectly polar.

XIV. MEASURING THE SHAPE OF THE POTENTIAL

The choice of the shape of the elastic potential seems to be a source of confusion to several people to whom we have presented this model, and a quadratic term in $\cos\phi$ has often been suggested. In a quadratic term, the dielectric response could be included for square-wave switching. The main reasons for not using a quadratic potential is that it would not reproduce the experimental behavior in our samples, and it does not remove the singular behavior that we have discussed in Sec. V. However, it would be useful to have a method to measure the shape of the elastic potential, since this would make the evaluation of different surface treatments easier. Here we want to show that such a measurement is possible. Suppose that we know the strength of the polarization and the thickness of our sample, and let us assume as earlier that we can use one single value of ϕ to represent the direction of the spontaneous polarization. Let the elastic force be the function $K(\phi)$, and assume that the viscosity also is a function $\gamma(\phi)$. We then get the differential equation

$$-PE\sin\phi + K(\phi) = \gamma(\phi)\dot{\phi} \ . \tag{33}$$

By measuring the current I as a function of time, the charge on the capacitor plates is easily calculated as

$$Q(t) = \int I(t)dt \ , \tag{34}$$

and it should not be difficult to find the right integration constant. From this we know the value of ϕ as a function of time, since

$$Q(t) = AP\cos\phi(t) \ . \tag{35}$$

Then we can also easily calculate $\dot{\phi}$, and thus we know everything in the differential equation (33) except the elastic force and the viscosity. Since we get two equations for each value of ϕ, one for switching up and one for switching down, it should be possible to solve these equations for $K(\phi)$ and $\lambda(\phi)$, and we can thus get information both about the elastic and the inelastic behavior of our sample. By varying the shape of the applied voltage, it should in principle also be possible to evaluate the contribution of the dielectric anisotropy. The difficulty in these measurements will be to find the best shape of the applied voltage; if the electric field is too strong, it will be difficult to resolve the elastic contribution. If, on the other hand, it is too weak, movement of disclination lines and elastic relaxation parallel to the boundaries will be important for the polarization reversal process, and then our approximations are no longer valid.

ACKNOWLEDGMENTS

This work has been supported by the National Swedish Board for Technical Development under Grants No. 84-3691 and No. 84-3638, by the Swedish Work Environment Fund under Grant No. 82-0822, by the Swedish National Science Research Council under Grant No. 84-3693, and by Asea Research and Innovation.

[1]I. Dahl and S. T. Lagerwall, Ferroelectrics **58**, 215 (1984).
[2]N. A. Clark and S. T. Lagerwall, Appl. Phys. Lett. **36**, 899 (1980).
[3]M. Glogarova and J. Pavel, J. Phys. (Paris) **45**, 143 (1984).
[4]Ph. Martinot-Lagarde, J. Phys. (Paris) Lett. **38**, L17 (1977).
[5]S. Garoff and R. B. Meyer, Phys. Rev. Lett. **38**, 848 (1977).
[6]P. Schiller, Cryst. Res. Technol. **21**, 301 (1986).
[7]K. Skarp, I. Dahl, S. T. Lagerwall, and B. Stebler, Mol. Cryst. Liq. Cryst. **114**, 283 (1984).
[8]N. A. Clark, M. A. Handschy, and S. T. Lagerwall, Mol. Cryst. Liq. Cryst. **94**, 213 (1983).
[9]M. Nakagawa and T. Akahane, J. Phys. Soc. Jpn. **55**, 1516 (1986).
[10]K. Okano, Jpn. J. Appl. Phys. **25**, L846 (1986).

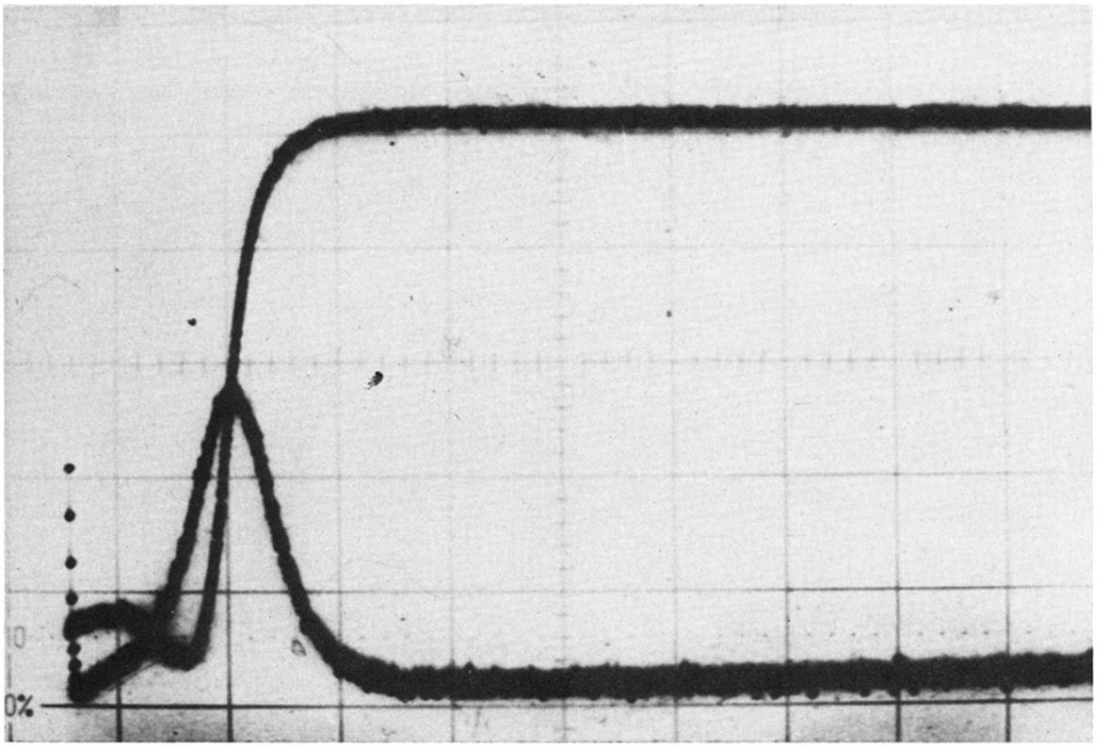

FIG. 6. An oscilloscope picture displaying the time coincidence between the electrical (current bump) and optical response (*S*-shaped curve).